AIP The Journal of Chemical Physics

Theoretical study of noble-gas containing metal halides

Chun-Hao Mou and Henryk A. Witek

Citation: The Journal of Chemical Physics **129**, 244310 (2008); doi: 10.1063/1.3043823
View online: http://dx.doi.org/10.1063/1.3043823
View Table of Contents: http://scitation.aip.org/content/aip/journal/jcp/129/24?ver=pdfcov
Published by the AIP Publishing

Theoretical study of noble-gas containing metal halides

Chun-Hao Mou[1] and Henryk A. Witek[1,2,a)]
[1]*Department of Applied Chemistry, National Chiao Tung University, Hsinchu 30010, Taiwan*
[2]*Institute of Molecular Science, National Chiao Tung University, Hsinchu 30010, Taiwan*

(Received 22 March 2007; accepted 17 November 2008; published online 31 December 2008)

Equilibrium structures, energetic stability, and vibrational frequencies of noble-gas containing metal halides, MNgX and NgMX (Ng=Ar, Kr, Xe; M=Cu, Ag, Au; X=F, Cl, Br) have been studied computationally using coupled cluster, density functional, and perturbation techniques. The NgMX species have been found to be stable with the Ng–M bond dissociation energy of 2–22 kcal/mol. Our calculations indicate that the argon-containing MNgX compounds are unstable or very weakly bound. For most of the krypton- and xenon-containing species, well-defined $(MNg)^{\delta+}X^{\delta-}$ equilibrium structures have been located. Large MNgX→Ng+MX reorganization barriers for some of the MNgX molecules (e.g., AuXeF and AuXeCl) indicate their considerable kinetic stability. The presented results suggest that direct observation of the most stable of the MNgX molecules might be possible in experiment. © *2008 American Institute of Physics*. [DOI: 10.1063/1.3043823]

I. INTRODUCTION

Since the discovery of noble gases,[1] the chemical community had been fascinated with the idea of stable chemical molecules containing atoms of these inert elements. Obviously, this interest was stimulated by the fact that the existence of such molecules would contradict generally accepted rules used to describe and analyze the stability of chemical species. For a long time, all experimental efforts to synthesize noble-gas containing compounds were unsuccessful.[2] Finally, in 1962 Bartlett succeeded in preparing $XePtF_6$.[3] Soon, many other xenon-containing compounds were identified experimentally.[4] The first stable compound of the heaviest noble gas, radon fluoride, was prepared in 1962.[5] Although radon was shown to react spontaneously with a number of molecules and complexes,[6] the practical importance of this discovery was rather limited owing to its high radioactivity. The first stable compound of krypton (KrF_2) was obtained in 1963.[7] It took a substantially longer time before the first stable compound of argon could be found;[8] argon fluorohydride (HArF) was observed[9] in 2000 using a low-temperature matrix-isolation technique developed in Räsänen group.[10–13] Most molecules prepared in that way have the H–Ng–X structure, where Ng is a noble-gas atom and X is an electronegative atom or group. Recently, more complicated structures, such as FNgBO, FNgCCH, or $FNgO^-$, were observed or theoretically predicted.[14–16] Although no stable compounds containing helium or neon have been characterized,[17,18] quantum chemical calculations suggest[8,19,20] that some of them could possibly be synthesized. At present, approximately five hundreds various compounds that contain noble-gas atoms are known; their detailed list can be found elsewhere.[18,21–24]

An interesting class of chemical compounds are the complexes of rare gases with transition-metal ions.[25–28] Many of such compounds, observed in experiment or investigated theoretically, have the NgMX structure.[29–41] It is natural to inquire if the noble gas atom can be inserted between the metal and the halogen. The resultant compounds would have the MNgX structure, which is a metal analog of the HNgX compounds observed in matrix-isolation studies.[10–13] Recently, a MP2 theoretical analysis of the structure and energetic stability of the MNgX-type compounds has been given by Ghanty.[42,43] His study, performed for some of the MNgF species (Ng=Ar, Kr, Xe; M=Cu, Ag, Au), shows that these molecules have metastable character. Ghanty also located a low-lying transition state leading the energetically favorable MF+Ng fragmentation.

In the present study, we use a spectrum of quantum chemical methods—CCSD(T), MP2, and DFT—to perform a systematic analysis of geometric structure and energetic stability of the MNgX and NgMX compounds (M=Cu, Ag, Au; Ng=Ar, Kr, Xe; X=F, Cl, Br). To understand the properties and the thermodynamic and kinetic stability of these species, two possible dissociation channels: (i) MNgX→M+Ng+X and (ii) MNgX→MX+Ng, are investigated together with the energy barrier for the reorganization reaction MNgX→Ng+MX. The technical details of our calculations are described in the next section. Section III presents the results and a discussion of these results is found in Sec. IV. The conclusions are given in the last section.

II. COMPUTATIONAL DETAILS

Two different basis sets/Hamiltonian schemes have been used to account for the relativistic effects. The first scheme—abbreviated later as ECP—employs the Stuttgart/Dresden (SDD) basis sets[44,45] with the corresponding effective core potentials (ECPs) for the Ar, Kr, Xe, Cu, Ag, and Au atoms. The basis sets for transition metals have been augmented with additional two f and one g polarization functions.[46] The resulting contraction schemes can be described as $(6s6p3d1f)/[4s4p3d1f]$ for rare gases and $(8s7p6d2f1g)/[6s5p3d2f1g]$ for metals. For halogens

a)Electronic mail: hwitek@mail.nctu.edu.tw.

TABLE I. Calculated equilibrium bond distances (in Å) for the MNgX species. All structures are linear. Structures denoted as … could not be found.

	r_{M-Ng}						r_{Ng-X}					
	MP2		B3LYP		CCSD(T)		MP2		B3LYP		CCSD(T)	
Molecule	ECP	DKH	ECP	DKH	ECP	DKH	ECP	DKH	ECP	DKH	ECP	DKH
CuArF	2.154	2.131	2.241	2.228	2.257	2.213	2.267	2.251	2.238	2.237	2.238	2.222
CuArCl	2.186	2.160	2.304	2.287	2.383[a]	2.322	2.768	2.751	2.768	2.767	2.726[a]	2.723
CuArBr	2.201	2.173	2.335	2.316	…	…	2.911	2.886	2.932	2.923	…	…
AgArF	2.413	2.399	2.532	2.529	…	…	2.302	2.288	2.282	2.286	…	…
AgArCl	2.455	2.438	2.616	2.612	…	…	2.798	2.781	2.823	2.827	…	…
AgArBr	2.476	2.457	2.655	2.650	…	…	2.934	2.909	2.991	2.986	…	…
AuArF	2.338	2.320	2.475	2.448	…	…	2.062	2.048	2.164	2.153	…	…
AuArCl	2.445	2.410	2.580	2.548	…	…	2.484	2.474	2.691	2.675	…	…
AuArBr	2.546	2.493	2.628	2.594	…	…	2.589	2.574	2.853	2.828	…	…
CuKrF	2.265	2.240	2.337	2.324	2.345	2.305	2.248	2.235	2.242	2.241	2.250	2.231
CuKrCl	2.291	2.264	2.385	2.370	2.396	2.351	2.772	2.754	2.788	2.784	2.773	2.748
CuKrBr	2.305	2.276	2.409	2.392	2.472	2.398	2.922	2.899	2.953	2.942	2.935	2.920
AgKrF	2.503	2.488	2.598	2.596	2.606	2.573	2.268	2.255	2.270	2.273	2.259	2.246
AgKrCl	2.538	2.521	2.663	2.659	2.664[a]	2.699	2.792	2.771	2.826	2.826	2.768[a]	2.774
AgKrBr	2.556	2.538	2.695	2.689	…	…	2.935	2.910	2.996	2.987	…	…
AuKrF	2.426	2.409	2.531	2.507	…	2.576[a]	2.049	2.042	2.154	2.146	…	2.182[a]
AuKrCl	2.487	2.465	2.601	2.572	…	…	2.502	2.490	2.683	2.669	…	…
AuKrBr	2.529	2.503	2.634	2.603	…	…	2.635	2.621	2.845	2.823	…	…
CuXeF	2.418	2.392	2.480	2.467	2.485	2.446	2.271	2.233	2.281	2.255	2.289	2.249
CuXeCl	2.435	2.408	2.511	2.497	2.515	2.473	2.828	2.795	2.855	2.834	2.851	2.815
CuXeBr	2.445	2.417	2.529	2.515	2.540	2.494	2.991	2.951	3.030	3.001	3.018	2.988
AgXeF	2.641	2.619	2.721	2.710	2.716	2.679	2.275	2.237	2.295	2.273	2.292	2.256
AgXeCl	2.667	2.642	2.768	2.755	2.767	2.725	2.831	2.801	2.878	2.861	2.854	2.824
AgXeBr	2.680	2.656	2.791	2.779	2.822	2.763	2.990	2.953	3.055	3.031	3.029	3.001
AuXeF	2.559	2.530	2.648	2.618	2.641	2.589	2.125	2.094	2.200	2.168	2.194	2.153
AuXeCl	2.593	2.559	2.692	2.654	2.713	2.643	2.603	2.578	2.743	2.716	2.743	2.703
AuXeBr	2.614	2.576	2.715	2.674	2.711[a]	2.682	2.752	2.725	2.915	2.878	2.911[a]	2.901

[a]No BSSE correction.

(F, Cl, Br), we have used the augmented correlation-consistent polarized valence triple-zeta (aug-cc-pVTZ) basis sets.[47–50] The second scheme—abbreviated later as DKH—has used all-electron basis sets with a fifth-order Douglas-Kroll-Hess Hamiltonian in McWeeny parametrization.[51,52] The relativistic all-electron basis sets are of the QZP (quadruple zeta plus polarization) quality; they were constructed by Roos and coworkers[53,54] using the second-order Douglas–Kroll–Hess Hamiltonian.[55,56]

The equilibrium structures, harmonic vibrational frequencies, and relative energies have been calculated using the CCSD(T),[57] MP2,[58] and DFT[59] methods. In the DFT calculations, the B3LYP functional[60,61] has been used. In the MP2/ECP and CCSD(T)/ECP calculations the following inner shells have not been correlated: [He] for F, [Ne] for Cl, and [Ar] for Cl. In the MP2/DKH and CCSD(T)/DKH calculations the following inner shells have not been correlated: [He] for F, [Ne] for Cl, [Ar] for Cl, [Ne] for Ar, [Ar] 3*d* for Kr, [Kr] 4*d* for Xe, [Ar] for Cu, [Kr] for Ag, and [Xe] for Au. The calculations have been performed using the GAUSSIAN 03 program package[62] and the MOLPRO program.[63] The basis set superposition error (BSSE) has been accounted for using standard counterpoise correction technique.[64] The counterpoise-corrected energies have been used to construct potential energy surfaces (PESs) in the vicinity of the equilibrium geometry for each of the studied molecules. Subsequently, we have employed these PESs to find BSSE-corrected values of equilibrium geometry parameters and harmonic vibrational frequencies using numerical differentiation. The CCSD(T) and MP2 energies of separated atoms have been calculated using single-determinant self-consistent field (SCF) wave functions as a reference. This approach is suitable for the noble gases (configuration p^6) and metal atoms (configuration s^1d^{10}), but it violates the atomic spherical symmetry for the halogen atoms (configuration s^2p^5). To estimate the corresponding symmetry-breaking error, we have employed additional multiconfigurational SCF calculations averaging the three spatial components of the atomic ^2P term of halogens. The resultant set of atomic orbitals with proper degeneracy has been subsequently used to calculate the MP2 and CCSD(T) energies. In all the considered cases the symmetry-breaking error has been found to be smaller than 0.05 kcal/mol and it has been disregarded.

III. RESULTS

Optimized CCSD(T), MP2, and DFT equilibrium structures for all the studied MNgX and NgMX molecules are

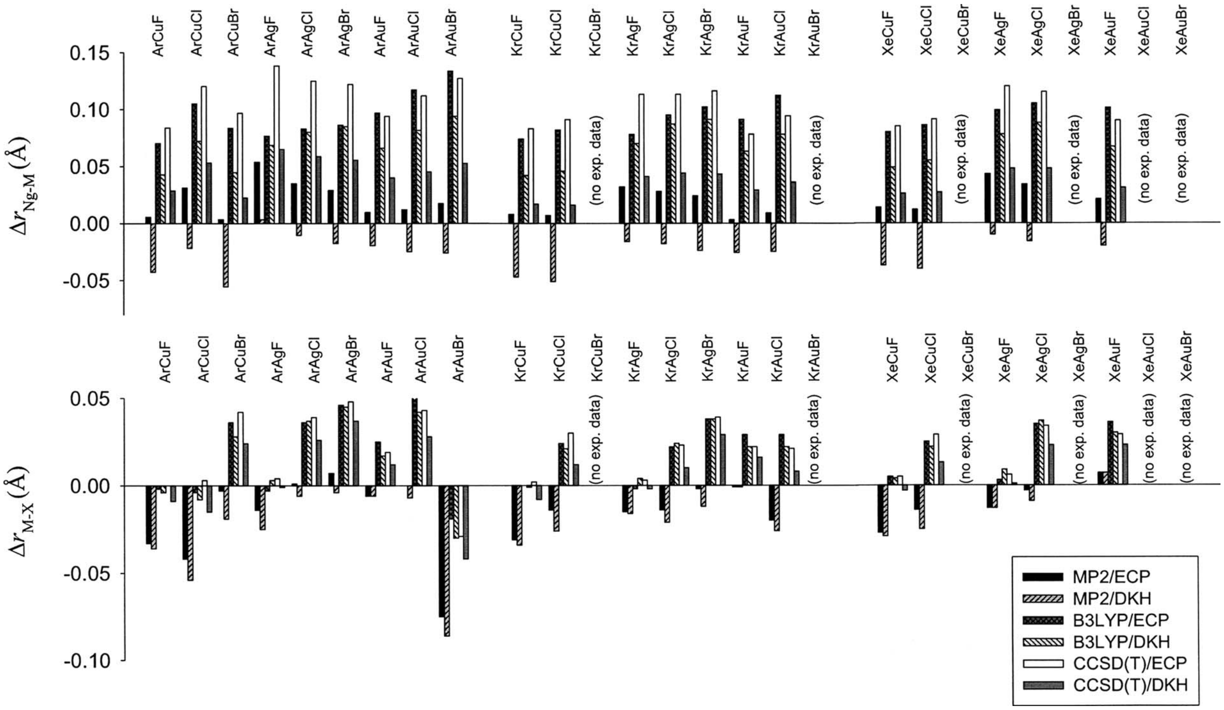

FIG. 1. Distribution of errors to experiment for the $r_{\text{Ng-M}}$ and $r_{\text{M-X}}$ bonds in NgMX.

TABLE II. Calculated equilibrium bond distances (in Å) for the NgMX species. All structures are linear.

	$r_{\text{Ng–M}}$							$r_{\text{M–X}}$						
	MP2		B3LYP		CCSD(T)			MP2		B3LYP		CCSD(T)		
Molecule	ECP	DKH	ECP	DKH	ECP	DKH	Expt.	ECP	DKH	ECP	DKH	ECP	DKH	Expt.
ArCuF	2.225	2.176	2.289	2.262	2.303	2.248	2.219	1.720	1.717	1.751	1.749	1.753	1.744	1.753
ArCuCl	2.278	2.225	2.352	2.319	2.367	2.300	2.247	2.036	2.024	2.074	2.070	2.081	2.063	2.078
ArCuBr	2.303	2.244	2.383	2.344	2.396	2.322	2.299	2.163	2.147	2.202	2.194	2.208	2.190	2.166
ArAgF	2.612	2.561	2.635	2.627	2.696	2.623	2.558	1.972	1.961	1.983	1.989	1.990	1.985	1.986
ArAgCl	2.647	2.602	2.695	2.692	2.737	2.671	2.612	2.269	2.262	2.304	2.305	2.307	2.294	2.268
ArAgBr	2.671	2.625	2.728	2.727	2.764	2.698	2.642	2.385	2.374	2.424	2.423	2.426	2.415	2.378
ArAuF	2.401	2.372	2.488	2.457	2.485	2.431	2.391	1.912	1.912	1.943	1.935	1.937	1.930	1.918
ArAuCl	2.481	2.444	2.586	2.551	2.581	2.514	2.469	2.198	2.191	2.248	2.240	2.241	2.226	2.198
ArAuBr	2.520	2.476	2.636	2.596	2.629	2.555	2.502	2.316	2.305	2.372	2.361	2.362	2.349	2.391
KrCuF	2.326	2.271	2.392	2.360	2.401	2.335	2.318	1.723	1.720	1.754	1.753	1.756	1.746	1.754
KrCuCl	2.370	2.312	2.445	2.409	2.454	2.379	2.363	2.039	2.027	2.077	2.074	2.083	2.065	2.053
KrCuBr	2.388	2.327	2.469	2.430	2.477	2.396	…	2.167	2.150	2.205	2.198	2.212	2.193	…
KrAgF	2.633	2.585	2.679	2.671	2.714	2.642	2.601	1.969	1.968	1.982	1.988	1.987	1.982	1.984
KrAgCl	2.671	2.625	2.738	2.730	2.756	2.687	2.643	2.268	2.261	2.304	2.306	2.305	2.292	2.282
KrAgBr	2.692	2.644	2.770	2.759	2.784	2.711	2.668	2.383	2.373	2.423	2.423	2.424	2.414	2.385
KrAuF	2.466	2.437	2.554	2.526	2.541	2.492	2.463	1.917	1.917	1.947	1.940	1.940	1.934	1.918
KrAuCl	2.532	2.498	2.635	2.601	2.617	2.559	2.523	2.203	2.197	2.252	2.245	2.244	2.231	2.223
KrAuBr	2.560	2.523	2.674	2.635	2.653	2.590	…	2.321	2.311	2.376	2.366	2.365	2.354	…
XeCuF	2.447	2.396	2.513	2.482	2.518	2.459	2.433	1.727	1.725	1.759	1.758	1.759	1.751	1.754
XeCuCl	2.484	2.432	2.558	2.527	2.563	2.499	2.472	2.044	2.033	2.083	2.080	2.087	2.071	2.058
XeCuBr	2.499	2.444	2.576	2.544	2.581	2.513	…	2.171	2.155	2.211	2.204	2.215	2.198	…
XeAgF	2.706	2.653	2.762	2.741	2.783	2.711	2.663	1.967	1.967	1.983	1.989	1.986	1.981	1.980
XeAgCl	2.745	2.695	2.816	2.799	2.826	2.759	2.711	2.268	2.262	2.306	2.308	2.305	2.294	2.271
XeAgBr	2.763	2.713	2.840	2.824	2.847	2.780	…	2.384	2.374	2.426	2.426	2.424	2.416	…
XeAuF	2.569	2.528	2.649	2.615	2.638	2.579	2.548	1.925	1.925	1.954	1.948	1.947	1.941	1.918
XeAuCl	2.626	2.580	2.719	2.677	2.701	2.636	…	2.213	2.208	2.261	2.254	2.253	2.240	…
XeAuBr	2.647	2.599	2.749	2.703	2.728	2.657	…	2.330	2.321	2.384	2.375	2.373	2.363	…

TABLE III. Calculated atomization energies (in kcal/mol) for the MNgX species. ZPE and BSSE corrections are included. The energy of the ionic dissociation limit ($M^{+}+Ng+X^{-}$) is given for comparison. Structures denoted as … could not be found.

	MP2		B3LYP		CCSD(T)	
Molecule	ECP	DKH	ECP	DKH	ECP	DKH
CuArF	−7.51	−4.20	−13.21	−14.37	−3.83	−4.90
CuArCl	4.44	9.50	−5.02	−5.99	−0.34[a]	2.40
CuArBr	10.06	11.93	−1.29	−2.05	…	…
AgArF	0.32	3.99	−8.68	−10.12	…	…
AgArCl	10.72	15.45	−2.11	−3.23	…	…
AgArBr	15.88	17.87	1.11	0.17	…	…
AuArF	20.48	22.99	1.63	0.71	…	…
AuArCl	30.42	34.23	8.02	7.41	…	…
AuArBr	32.69	33.79	10.40	9.88	…	…
CuKrF	−20.34	−20.62	−23.79	−25.19	−15.70	−21.92
CuKrCl	−5.49	−4.71	−12.53	−13.79	−4.77	−11.33
CuKrBr	0.62	−1.22	−8.09	−9.15	−1.29	−7.48
AgKrF	−11.91	−11.78	−18.20	−19.57	−9.85	−15.77
AgKrCl	1.56	2.48	−8.42	−9.73	−5.32[a]	−8.61[a]
AgKrBr	7.20	5.43	−4.48	−5.62	…	…
AuKrF	−2.01	−2.70	−12.48	−14.22	…	−14.17[a]
AuKrCl	12.87	13.03	−1.72	−3.16	…	…
AuKrBr	17.11	14.58	1.77	0.46	…	…
CuXeF	−37.50	−42.71	−37.70	−40.62	−31.59	−40.28
CuXeCl	−18.20	−21.80	−22.15	−24.09	−16.06	−24.65
CuXeBr	−11.31	−17.70	−16.76	−18.66	−11.49	−19.89
AgXeF	−29.03	−34.17	−31.49	−34.40	−25.23	−33.63
AgXeCl	−10.82	−14.36	−17.11	−19.15	−10.83	−19.38
AgXeBr	−4.34	−10.71	−12.15	−13.95	−6.76	−15.24
AuXeF	−28.34	−35.56	−31.15	−35.75	−24.91	−35.99
AuXeCl	−7.89	−13.24	−15.07	−18.56	−9.49	−20.09
AuXeBr	−1.89	−10.00	−10.20	−13.40	−11.44[a]	−16.09
$Cu^{+}+Ng+F^{-}$	91.00	97.12	109.05	108.88	96.66	100.67
$Cu^{+}+Ng+Cl^{-}$	91.20	98.40	105.61	106.07	92.19	96.28
$Cu^{+}+Ng+Br^{-}$	94.53	99.28	108.62	109.52	94.77	96.17
$Ag^{+}+Ng+F^{-}$	88.32	93.25	102.44	100.47	94.13	96.20
$Ag^{+}+Ng+Cl^{-}$	88.52	94.53	99.00	97.65	89.66	91.81
$Ag^{+}+Ng+Br^{-}$	91.85	95.41	102.01	101.11	92.24	91.70
$Au^{+}+Ng+F^{-}$	128.27	133.33	136.04	137.40	130.51	132.43
$Au^{+}+Ng+Cl^{-}$	128.47	134.61	132.60	134.59	126.05	128.03
$Au^{+}+Ng+Br^{-}$	131.80	135.49	135.62	138.04	128.63	127.92

[a]No BSSE correction.

given in Tables I and II, respectively. For NgMX, available experimental bond lengths are also given. As expected,[29–43] both types of molecules (MNgX and NgMX) have linear structures. At the MP2 and DFT level, all the considered species are found to possess well-defined energy minima. At the CCSD(T) level, the equilibrium geometry for some of the MNgX compounds could not be found owing to the breakdown within the CCSD(T) computational scheme. More detailed discussion of this phenomenon is given in Sec. IV. The effect of using different basis set and Hamiltonian schemes (ECP versus DKH) does not seem to have a very strong effect on the calculated geometric parameters. The largest difference between the ECP and DKH bond lengths is 0.081 Å, while in most cases the difference is not larger than 0.03 Å (except for the Ng–M bonds at the CCSD(T) level, where the difference systematically is about 0.07 Å). The characteristic features of the optimized structures of the MNgX and NgMX compounds are discussed below.

The M–Ng bonds in the MNgX-type species are usually shorter than those in the NgMX-type structures. In MNgX we can observe an additional ionic interaction between partially charged M and X atoms, leading to a further shortening of the M–Ng bond. This effect is most distinct for silver species. All methods give a consistent picture of this phenomenon. The M–Ng bonds in MNgX and NgMX are longest for silver and shortest for copper. The Au–Ng bonds are shorter than the corresponding Ag–Ng bonds owing to a strong relativistic contraction of the gold atom.[65] A similar effect is observed experimentally for the AgH (r_e=1.618 Å) and AuH (r_e=1.524 Å).[65] In general, the

TABLE IV. Calculated atomization energies (in kcal/mol) for the NgMX and MX species. ZPE and BSSE corrections are included. The atomization energy of the MX species is given for comparison.

	MP2		B3LYP		CCSD(T)	
Molecule	ECP	DKH	ECP	DKH	ECP	DKH
ArCuF	−110.74	−108.54	−98.95	−101.85	−99.48	−102.66
ArCuCl	−93.72	−90.88	−85.07	−87.46	−85.82	−89.89
ArCuBr	−85.12	−85.46	−77.71	−79.83	−78.94	−81.96
ArAgF	−86.56	−82.64	−79.46	−81.05	−80.13	−80.89
ArAgCl	−76.15	−71.55	−70.22	−71.52	−71.46	−73.41
ArAgBr	−70.08	−68.41	−64.73	−65.78	−66.37	−67.58
ArAuF	−78.24	−74.63	−73.01	−75.50	−71.70	−74.57
ArAuCl	−71.77	−68.26	−66.11	−68.53	−65.94	−70.29
ArAuBr	−66.54	−65.82	−61.35	−63.42	−61.69	−64.09
KrCuF	−113.54	−114.81	−101.00	−104.19	−101.75	−110.06
KrCuCl	−96.23	−97.65	−87.02	−89.90	−87.99	−97.14
KrCuBr	−87.63	−91.67	−79.59	−81.96	−81.06	−89.09
KrAgF	−88.97	−88.29	−81.51	−83.15	−82.10	−87.83
KrAgCl	−78.43	−77.31	−72.02	−73.33	−73.28	−80.09
KrAgBr	−72.25	−74.04	−66.39	−67.47	−68.09	−74.10
KrAuF	−83.13	−83.15	−76.56	−79.50	−75.65	−83.57
KrAuCl	−76.04	−76.05	−69.05	−71.69	−69.28	−78.66
KrAuBr	−70.55	−73.39	−64.02	−66.34	−64.74	−72.13
XeCuF	−117.36	−122.63	−104.18	−107.40	−105.11	−115.33
XeCuCl	−99.95	−105.40	−90.00	−92.91	−91.17	−102.29
XeCuBr	−91.30	−99.42	−82.48	−84.89	−84.15	−94.22
XeAgF	−92.58	−96.40	−84.50	−86.44	−85.06	−93.25
XeAgCl	−81.75	−84.99	−74.63	−76.13	−75.99	−85.16
XeAgBr	−75.44	−81.59	−68.84	−70.09	−70.66	−79.05
XeAuF	−89.75	−94.74	−81.69	−85.44	−81.21	−92.13
XeAuCl	−81.90	−86.81	−73.39	−76.78	−74.09	−86.37
XeAuBr	−76.20	−83.90	−68.09	−71.12	−69.30	−79.68
Ng+CuF	−102.50	−98.92	−91.35	−92.89	−92.60	−94.07
Ng+CuCl	−87.07	−83.83	−79.10	−80.45	−80.73	−82.88
Ng+CuBr	−79.20	−78.69	−72.51	−73.45	−74.41	−75.68
Ng+AgF	−83.10	−79.00	−76.01	−76.94	−77.45	−77.14
Ng+AgCl	−72.69	−68.38	−67.30	−68.16	−68.83	−69.89
Ng+AgBr	−66.82	−65.44	−62.19	−62.83	−63.93	−64.22
Ng+AuF	−67.65	−63.12	−65.35	−66.34	−64.46	−64.82
Ng+AuCl	−63.81	−59.64	−60.95	−62.15	−60.70	−63.13
Ng+AuBr	−59.75	−58.41	−57.23	−58.22	−57.35	−58.09

bonds between the metal atom and xenon in MNgX are longer than the bonds between the metal atom and krypton. Analogous to the case of the metal atom, the equilibrium distance between halogen and xenon in MNgX is larger than between halogen and krypton. The trend in the equilibrium distance d between the noble gas atom and the halogen atom in MNgX is $d_{\mathrm{Ng-Br}} > d_{\mathrm{Ng-Cl}} > d_{\mathrm{Ng-F}}$. These facts can be easily understood taking into account the increasing atomic radius for heavier halogens and noble gases. In the MNgX-type species, $d_{\mathrm{M-Ng}}$ depends much more strongly on the identity of the noble gas atom than $d_{\mathrm{Ng-X}}$. For example, the length of the Cu–Ng bond in CuNgF increases by 0.141 Å if krypton is substituted with xenon, while the length of the Ng–F bond increases only by 0.018 Å (CCSD(T)/DKH level). The M–Ng bond distances calculated using MP2 are consistently shorter than those obtained with B3LYP and CCSD(T) by approximately 0.05–0.1 Å.

Energetic stability of the MNgX, NgMX, and MX+Ng species has been analyzed by comparing their energies—including BSSE and ZPE corrections–with the energy of the gas-phase atomization limit: M+Ng+X. The calculated atomization energies of the MNgX species are presented in Table III together with the energies for the ionic dissociation limit $M^{+}+Ng+X^{-}$. The calculated atomization energies of the NgMX and MX species are given in Table IV. As previously discussed for geometries, energetics of some of the MNgX compounds at the CCSD(T) level could not be accessed owing to a break-down of the coupled-cluster scheme (for details, see Sec. IV). The largest computed energy difference between the ECP and DKH schemes is approximately 12 kcal/mol for CCSD(T), 8 kcal/mol for MP2, and 5 kcal/mol for B3LYP. The atomization energies computed with different methods can show large variation. The largest discrepancy is observed between MP2/DKH and B3LYP/

TABLE V. Calculated ECP structures and barrier heights of the transition state for the $MNgX \rightarrow MX + Ng$ reorganization reaction. Structures denoted as … could not be found. Bond lengths r are given in Å, angles α in degrees, and the barrier heights $\Delta V^{\ddagger}$ in kcal/mol. The BSSE corrections are included only for the MP2 method.

	r_{M-Ng}			r_{Ng-X}			α_{M-Ng-X}			$\Delta V^{\ddagger}$		
Molecule	MP2	B3LYP	CCSD(T)	MP2	B3LYP	CCSD(T)	MP2	B3LYP	CCSD(T)	MP2	B3LYP	CCSD(T)
CuArF	2.155	2.259	2.180	2.347	2.447	2.347	138.4	113.2	129.1	1.02	5.45	1.96
CuArCl	2.185	2.323	…	2.823	2.953	…	146.9	120.3	…	0.31	2.96	…
CuArBr	2.198	2.357	…	2.970	3.118	…	146.5	121.0	…	0.34	2.61	…
AgArF	2.415	2.566	…	2.364	2.472	…	144.9	117.5	…	0.46	3.77	…
AgArCl	2.454	2.651	…	2.835	2.979	…	154.1	126.1	…	0.08	1.86	…
AgArBr	2.472	2.698	…	2.979	3.151	…	152.2	126.3	…	0.15	1.56	…
AuArF	2.339	2.593	…	2.349	2.511	…	121.9	106.0	…	8.45	9.67	…
AuArCl	2.396	2.733	…	2.812	3.023	…	122.2	111.0	…	7.93	5.33	…
AuArBr	2.457	2.803	…	2.947	3.177	…	119.5	113.4	…	9.54	4.46	…
CuKrF	2.262	2.349	2.276	2.427	2.526	2.421	121.1	103.4	116.5	5.39	11.32	7.71
CuKrCl	2.287	2.409	2.311	2.934	3.071	2.940	127.3	109.1	121.5	3.04	6.94	4.88
CuKrBr	2.296	2.438	2.342	3.088	3.240	3.101	127.7	110.3	120.0	2.95	6.25	5.15
AgKrF	2.504	2.632	2.524	2.441	2.556	2.438	124.7	105.1	116.9	4.23	9.15	7.68
AgKrCl	2.535	2.712	2.592	2.943	3.099	2.951	131.4	111.8	120.2	2.24	5.13	5.08
AgKrBr	2.547	2.750	…	3.095	3.267	…	131.3	113.4	…	2.28	4.54	…
AuKrF	2.416	2.633	…	2.429	2.609	…	110.2	96.1	…	19.37	19.06	…
AuKrCl	2.450	2.735	…	2.932	3.143	…	112.3	101.9	…	16.16	11.72	…
AuKrBr	2.472	2.793	…	3.082	3.303	…	111.1	103.6	…	17.15	10.24	…
CuXeF	2.396	2.454	2.407	2.503	2.594	2.490	110.1	94.4	107.5	11.92	18.74	13.86
CuXeCl	2.418	2.514	2.434	3.077	3.232	3.083	115.9	100.0	112.6	7.41	12.30	9.15
CuXeBr	2.424	2.539	2.448	3.247	3.421	3.255	116.6	101.1	112.1	7.04	11.25	9.13
AgXeF	2.629	2.728	2.640	2.521	2.636	2.509	111.7	95.3	107.7	11.19	17.07	14.10
AgXeCl	2.655	2.802	2.676	3.089	3.262	3.096	118.0	101.6	112.3	6.78	10.48	9.43
AgXeBr	2.663	2.835	2.703	3.258	3.447	3.267	118.5	102.8	111.0	6.55	9.41	9.52
AuXeF	2.530	2.693	2.563	2.501	2.717	2.496	102.1	87.2	97.6	30.12	30.85	31.66
AuXeCl	2.549	2.779	…	3.080	3.339	…	104.8	93.5	…	24.49	20.36	…
AuXeBr	2.557	2.820	…	3.252	3.526	…	104.4	94.9	…	24.85	18.25	…

DKH for AuArCl (26.8 kcal/mol). Large variation may suggest that the computed energetics is not very accurate, having an error of approximately 10 kcal/mol or larger. The characteristic features observed for the computed energetics of the MNgX and NgMX species are discussed below.

All the NgMX-type structures are considerably more stable then the corresponding MNgX-type species. This fact is mainly attributed to a very strong M–X bond in NgMX. Docking an additional noble gas atom to the positively charged metal in MX gives stabilization of only 2–22 kcal/mol, while dissociating the M–X bond requires as much as 57–103 kcal/mol. Two regularities can be observed for the MNgX-type molecules: (1) MNgX is thermodynamically more stable for heavier noble gas atoms ($Xe > Kr > Ar$); (2) MNgX is thermodynamically more stable for lighter M and X atoms ($Cu > Ag > Au$; $F > Cl > Br$). The calculated energies of some of the MNgX compounds (e.g., AuKrBr or most argon-containing structures) are higher than the corresponding limit of separated atoms. Their rather unexpected thermodynamic stability can be explained by a strong ionic character of interactions originating from a substantial electron transfer from metal to halogen. Therefore, they should rather be compared to the ionic dissociation limit, $M^{+} + Ng + X^{-}$, which is located much higher than the $M + Ng + X$ limit (see Table III). For example, the MP2/ECP ionic limit for CuArBr is 94.5 kcal/mol higher than the limit for the neutral atoms giving stabilization energy of 84.5 kcal/mol for this molecule. Of course, in practice the ionic dissociation limit may be never approached owing to an electron transfer between X^{-} and M^{+}. This naturally brings up a question about the kinetic stability of such endothermic compounds. Our attempts to locate the interatomic separation corresponding to such an electron transfer (and simultaneously determine the height of the corresponding energy barrier) have failed. The potential energy surface is very steep along the r_{MNg} and r_{NgX} coordinates in a large region around the equilibrium geometry that could be accessed with single-reference methods used in this study. This shows that the potential energy barrier is rather high and the MNgX species should be kinetically stable with respect to the $M + Ng + X$ dissociation process. A definitive answer to this issue must be sought with some multireference treatment that we plan to perform in the near future.

The data presented in Tables III and IV give information on thermodynamic and in part on kinetic stability of the MNgX and NgMX species. To complete the stability analysis, we have also considered the internal reorganization reaction $MNgX \rightarrow NgMX$ (or $Ng + MX$) and determined the corresponding transition state (TS). This reorganization corresponds to the bending of the MNgX molecule and may

TABLE VI. Calculated harmonic vibrational frequencies [in cm^{-1}] for the MNgX species. Structures denoted as … could not be found.

	ω_{sym}						ω_{asym}						ω_{bend}					
	MP2		B3LYP		CCSD(T)		MP2		B3LYP		CCSD(T)		MP2		B3LYP		CCSD(T)	
Molecule	ECP	DKH	ECP	DKH	ECP	DKH	ECP	DKH	ECP	DKH	ECP	DKH	ECP	DKH	ECP	DKH	ECP	DKH
CuArF	226	233	195	198	188	204	379	389	353	356	341	357	63	60	73	86	80	81
CuArCl	158	162	130	131	131[a]	95	312	323	258	261	238[a]	225	38	41	50	58	56[a]	57
CuArBr	117	121	94	95	…	…	289	301	229	233	…	…	36	39	39	51	…	…
AgArF	185	189	149	148	…	…	341	348	317	315	…	…	49	44	64	69	…	…
AgArCl	132	136	100	99	…	…	267	275	223	221	…	…	27	30	52	43	…	…
AgArBr	97	100	71	71	…	…	242	250	193	192	…	…	28	29	44	38	…	…
AuArF	204	212	153	158	…	…	376	389	364	369	…	…	131	138	99	104	…	…
AuArCl	135	143	98	101	…	…	253	265	246	251	…	…	95	99	70	66	…	…
AuArBr	86	95	68	70	…	…	212	225	210	215	…	…	84	88	60	57	…	…
CuKrF	234	240	202	204	201	212	330	335	327	327	330	339	82	88	84	88	82	91
CuKrCl	170	175	146	149	151	160	255	261	223	224	216	227	53	54	55	57	54	57
CuKrBr	123	126	105	107	91	108	237	244	198	201	166	181	47	48	49	49	44	47
AgKrF	184	188	153	151	142	151	310	314	307	304	318	324	72	97	70	74	75	92
AgKrCl	143	147	112	113	96[a]	74	219	224	195	195	202[a]	199	45	46	43	46	48[a]	47
AgKrBr	106	109	82	84	…	…	194	199	162	164	…	…	40	41	39	38	…	…
AuKrF	191	197	153	160	…	92[a]	392	399	354	359	…	337[a]	131	132	101	104	…	63[a]
AuKrCl	149	155	115	120	…	…	253	258	223	227	…	…	89	89	59	65	…	…
AuKrBr	112	117	85	89	…	…	206	212	183	188	…	…	74	75	51	54	…	…
CuXeF	228	230	201	199	201	207	342	350	337	340	341	350	94	119	96	93	89	95
CuXeCl	182	186	162	163	168	175	232	236	211	212	212	219	60	62	57	59	57	60
CuXeBr	128	132	116	117	122	126	219	222	190	189	181	190	52	53	49	50	48	50
AgXeF	174	176	147	148	150	155	332	340	325	326	336	342	87	77	88	84	82	104
AgXeCl	150	153	123	123	122	128	205	209	191	192	201	206	54	55	47	50	51	52
AgXeBr	114	118	96	96	87	97	175	178	155	155	150	156	45	46	41	41	40	42
AuXeF	177	184	148	156	147	161	424	438	372	383	383	395	124	131	111	108	105	86
AuXeCl	153	160	123	131	104	122	259	265	219	225	227	235	83	85	62	66	61	66
AuXeBr	126	131	98	104	78[a]	82	200	208	170	177	176[a]	177	67	69	51	53	48[a]	49

[a]No BSSE correction.

lead to two possible product channels: isomerization to NgMX or dissociation to MX+Ng. Our relaxed scan calculations (see Fig. S1 in Ref. 66) show that in fact the second channel is preferred. Geometric parameters for the ECP transition-state structures are presented in Table V together with the magnitude $\Delta V^{\ddagger}$ of the corresponding energy barriers. The BSSE corrections have been included only for the MP2 method; their magnitude is small (see Table T-VIII in Ref. 66) and does not seem to introduce large changes in the computed structures and energy barriers. The transition state has the form of an obtuse triangle with the $\alpha_{M\text{–}Ng\text{–}X}$ angle between 87.2° and 154.1°. The value of the angles for analogous structures containing chlorine and bromine are very similar. Similar tendencies in the length of the M–Ng and Ng–X bonds in TS can be observed in the MNgX-type species. The trend observed for the kinetic stability of the MNgX species (Xe>Kr>Ar; F>Cl≈Br; Au>Cu>Ag) with respect to the Ng+MX fragmentation is similar to the analogous trend for the NgMX species (See Table IV and Refs. 41 and 43). The height of the energy barrier corresponding to the transition state is usually small. Only for a few molecules (mostly xenon species), is it larger than 10.0 kcal/mol, which is probably sufficient to ensure their kinetic stability.

Vibrational spectroscopy is the main practical tool to identify various compounds of noble gases in experiment. Therefore, we present here harmonic vibrational frequencies computed for all the considered MNgX and NgMX species to facilitate the identification of these molecules in experiment. The computed MP2, B3LYP, and CCSD(T) harmonic vibrational frequencies of the MNgX species are shown in Table VI. Analogous results obtained for the NgMX species are given in Table VII together with a compilation of available experimental data. An interesting aspect of our calculations is the fact that the calculated frequencies are BSSE-free. The BSSE corrections can be quite large, especially for the ECP calculations (maximal correction is 35 cm^{-1} for ω_{sym} of ArCuF in the MP2/DKH calculations, see Ref. 66, Table T-X). Similar size of change can be expected if a different basis set/Hamiltonian model is employed: the maximal discrepancy between the ECP and DKH frequencies is 32 cm^{-1} for KrCuCl at the MP2 level. Again, harmonic vibrational frequencies computed with various methods may differ to a large extent. [See, for example, the value of ω_{asym} for CuArBr computed with MP2/DKH (300.7 cm^{-1}) and with B3LYP/DKH (233.2 cm^{-1})]. In general, the harmonic vibrational frequencies computed with the MP2 method differ quite strongly from those computed with CCSD(T) and

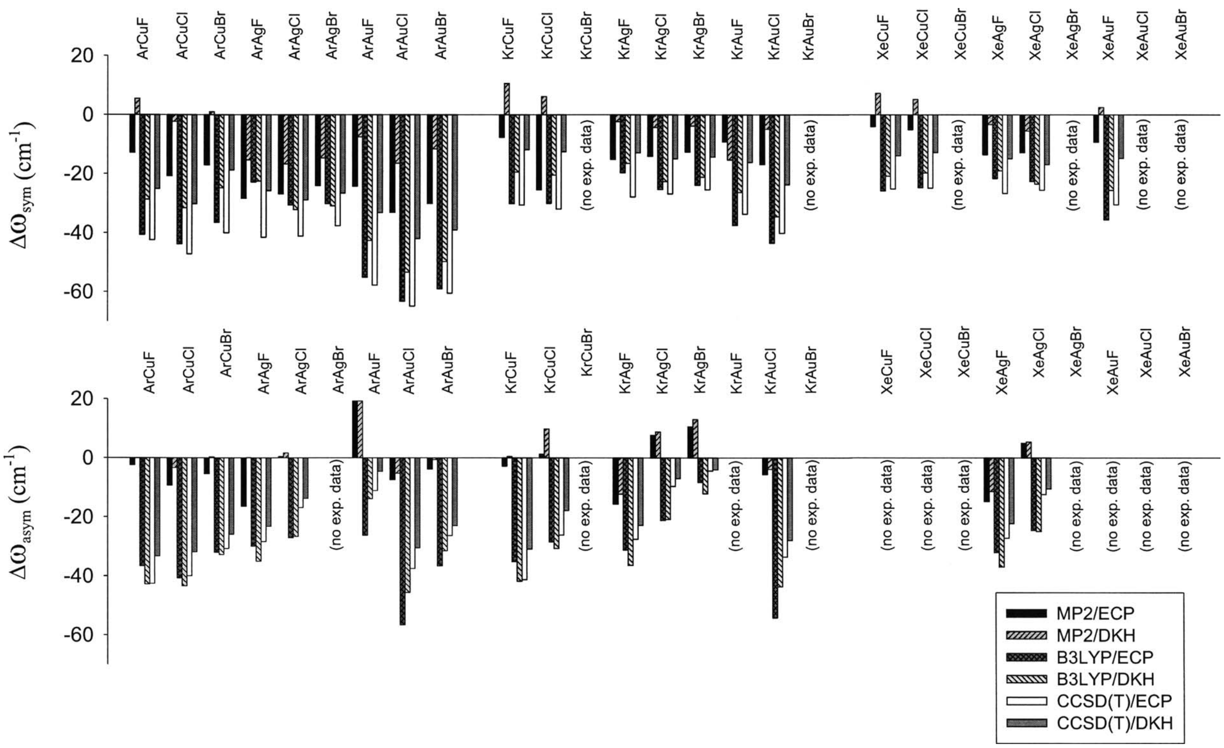

FIG. 2. Distribution of errors to experiment for the ω_{sym} and ω_{asym} harmonic vibrational frequencies in NgMX.

TABLE VII. Calculated harmonic vibrational frequencies (in cm^{-1}) for the NgMX species.

	ω_{sym}							ω_{asym}							ω_{bend}					
	MP2		B3LYP		CCSD(T)			MP2		B3LYP		CCSD(T)			MP2		B3LYP		CCSD(T)	
Molecule	ECP	DKH	ECP	DKH	ECP	DKH	Expt.	ECP	DKH	ECP	DKH	ECP	DKH	Expt.	ECP	DKH	ECP	DKH	ECP	DKH
ArCuF	211	229	183	195	182	199	224	672	674	637	631	631	641	674	127	131	132	112	106	112
ArCuCl	176	195	153	165	150	167	197	447	453	415	413	416	424	456	85	90	68	76	70	76
ArCuBr	153	171	134	145	130	151	170	345	350	318	317	319	324	350	70	73	57	64	58	64
ArAgF	113	126	118	119	99	115	141	525	541	511	506	513	518	541	63	64	82	62	56	72
ArAgCl	108	118	104	103	94	106	135	357	359	330	330	340	343	357	46	47	42	43	40	42
ArAgBr	100	109	94	93	86	97	124	263	266	246	242	248	249	…	38	39	40	35	32	34
ArAuF	197	213	166	178	163	188	221	602	602	557	569	572	578	583	123	142	94	111	108	113
ArAuCl	165	182	135	145	133	156	198	406	408	356	367	376	382	413	82	84	64	71	69	75
ArAuBr	148	166	119	128	117	139	178	282	285	249	255	260	263	286	64	67	58	55	53	59
KrCuF	177	196	155	166	154	173	185	666	669	634	627	628	638	669	120	130	131	106	102	102
RrCuCl	137	168	132	142	130	149	162	442	451	413	410	415	423	441	92	84	65	72	67	73
KrCuBr	129	145	114	122	111	129	…	343	350	317	316	318	324	…	65	70	57	60	55	60
KrAgF	110	123	105	108	97	112	125	528	532	513	508	516	521	544	69	90	84	65	61	70
KrAgCl	103	113	92	94	90	102	117	360	361	331	331	342	345	352	49	50	38	44	43	44
KrAgBr	93	102	82	85	81	92	106	266	268	247	243	251	251	255	39	40	36	35	34	35
KrAuF	167	161	139	150	142	160	176	600	599	555	566	572	577	…	107	116	87	107	106	112
KrAuCl	144	156	118	126	121	137	161	403	405	355	365	375	381	409	78	80	55	68	68	72
KrAuBr	131	143	104	114	108	124	…	281	283	249	253	260	262	…	60	61	48	52	51	55
XeCuF	174	185	152	157	153	164	178	662	663	630	622	626	633	…	115	120	130	101	99	107
XeCuCl	150	160	130	135	130	142	155	442	447	409	406	413	420	…	76	80	63	69	66	71
XeCuBr	127	136	110	115	110	121	…	343	347	315	313	318	322	…	62	66	55	58	54	58
XeAgF	116	127	108	111	103	115	130	531	535	514	509	519	524	546	71	83	87	69	66	90
XeAgCl	107	115	97	97	94	103	120	361	361	331	331	344	345	356	51	52	40	46	46	47
XeAgBr	96	102	86	85	84	92	…	267	269	248	243	252	252	…	41	42	37	37	36	37
XeAuF	160	171	133	143	139	154	169	592	592	550	559	567	572	…	115	119	87	105	105	108
XeAuCl	140	152	113	124	121	135	…	398	399	350	360	371	376	…	75	78	54	68	67	71
XeAuBr	129	140	103	112	110	124	…	277	279	246	250	257	259	…	57	59	48	51	50	54

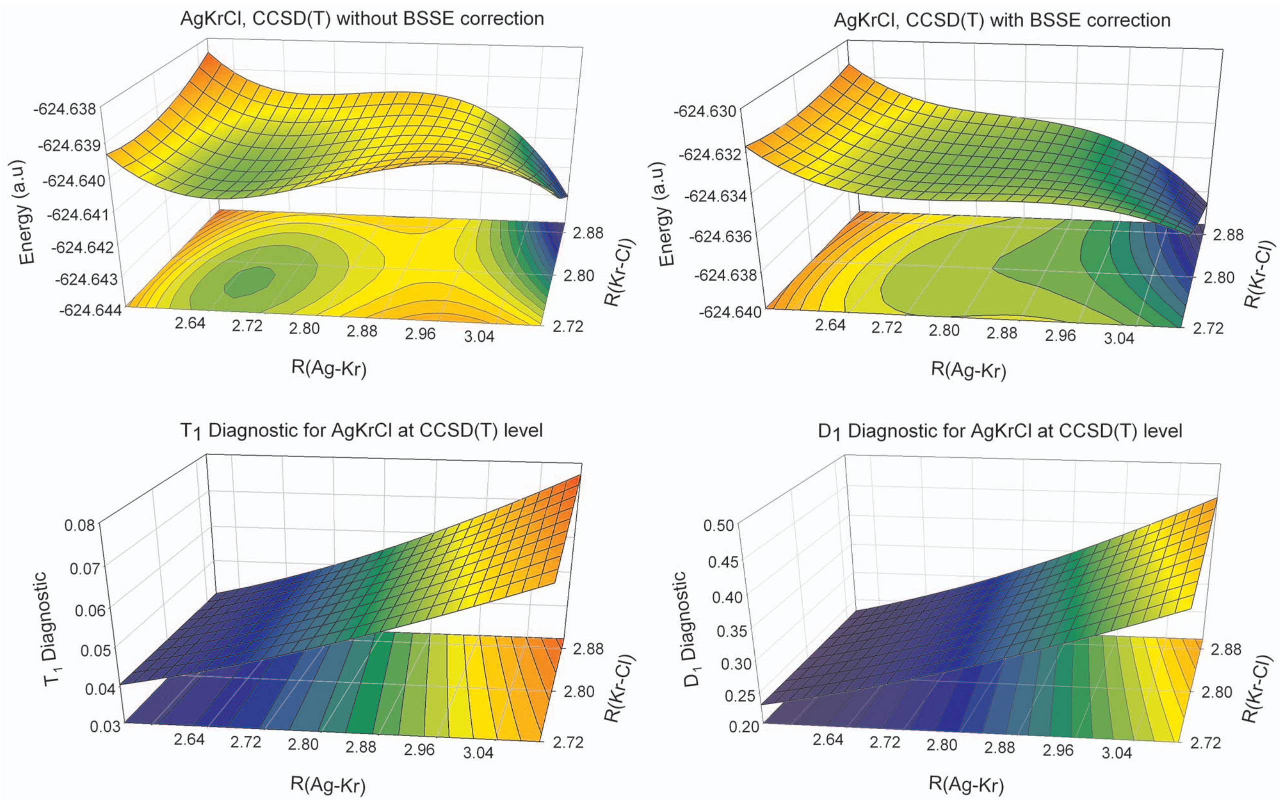

FIG. 3. (Color) 2D PES for AgKrCl computed at the CCSD(T)/ECP level with and without BSSE correction. Lower graphs show the values of the T_1 and D_1 diagnostics.

B3LYP. From the analysis shown in the next section, we may expect that the most accurate are the vibrational frequencies determined using the MP2/DKH and MP2/ECP methods. For the MNgX compounds, the computed harmonic vibrational frequencies ω_{sym} corresponding predominantly to the M–Ng stretch are between 68 and 240 cm^{-1}, those corresponding to the Ng–X stretch (ω_{asym}) are between 150 and 438 cm^{-1}, and those corresponding to the bending mode are between 28 and 138 cm^{-1}. All these values are rather small indicating weak bonding in these molecules. For the NgMX-type of structures, only the M–X stretch frequencies (ω_{asym}) are noticeably larger (between 242 and 674 cm^{-1}).

IV. DISCUSSION

The current study gives a systematic analysis of energetics, structures, and frequencies of a new class of the MNgX compounds. The presented MP2/ECP results correspond rather well to the previous theoretical predictions.[42,43] According to our results the kinetic stability of most of the argon-containing MNgX compounds is rather questionable. In general, the xenon-containing molecules are considerably more stable than their analogs containing krypton. At the CCSD(T) level, no equilibrium structure has been found for a number of MNgX species; reasons for this fact are discussed below. At the MP2 and B3LYP levels, minima for all of the structures have been located, but some of the corresponding MNgX→Ng+MX reorganization barriers are negligible, which suggests their kinetically unstable character. The most stable MNgX molecule is AuXeF with the AuXeF→Xe+AuF reorganization energy barrier of 31.7 kcal/mol [CCSD(T)/ECP] and the Au+Xe+F dissociation energy of 36.0 kcal/mol [CCSD(T)/DKH]. The most stable krypton-containing MNgX molecule is AuKrF with the reorganization energy barrier of 19.1 kcal/mol (B3LYP/ECP) and the atomization energy of 14.2 kcal/mol (B3LYP/DKH). The MArX molecule that has the largest chance to be detected experimentally is AuArF with the reorganization barrier of 9.7 kcal/mol (B3LYP/ECP). The presented energy estimates of the metastable MNgX compounds do not inform us about the actual lifetime of these species. It would be extremely interesting to perform wave-packet dynamics on a full-dimensional potential energy surface in an analogous way as it was done for HXeH.[67] This study showed that some of the vibrational levels of HXeH have surprisingly long lifetime (of order of nanoseconds) in gas phase, what suggests that this molecule can possibly be observed experimentally. We are planning to perform similar study for the most stable of the MNgX species; calculations of full-dimensional potential energy surfaces are in progress.

An important issue concerning our calculations is an estimation of the reliability of the obtained molecular parameters. Unfortunately, no close agreement is found between the results computed with all the employed quantum chemical methods that would allow us to gain more confidence about the accuracy of the presented data. This poses a natural question: which of the computational schemes employed in this study is actually reproducing the experimental findings in the best manner? To answer this question, we have compared our results with the available experimental data for the NgMX molecules; the experimental bond lengths and vibrational frequencies are taken from Refs. 29–39. The distribution of errors to experiment for the bond lengths is presented in Fig. 1. Analogous error distributions for the computed harmonic vibrational frequencies are given in Fig. 2. We have found that the M–X bond lengths are reproduced by all methods with similar mean absolute error of 0.015–0.025 Å. This is no longer true for the Ng–M bond lengths, for which the error can vary between 0.022 and 0.106 Å. The best correspondence to experiment is obtained with the MP2 method, used together either with the ECP or DKH basis set/Hamiltonian scheme. The mean absolute error in the r_{Ng-M} bonds is 0.022 and 0.025 Å, respectively. The reported experimental equilibrium distances correspond predominantly to geometries averaged over the zero-point vibrational levels (so called r_0 distances). On other hand, the computed equilibrium constants are the true equilibrium distances corresponding to a minimum on the potential energy surface (so called r_e distances). In general, the values of r_0 are usually larger than the values of r_e. For example, the r_0-r_e differences for the O–N, N=C, C–C, and C–H bonds in furazan ($C_2H_2N_2O$) are 0.007, 0.002, 0.006, and 0.001 Å, respectively.[68] For the molecules studied here, the difference can be actually larger owing to larger anharmonicities in the studied potential energy surfaces. Including this regularity in our analysis and examining the error pattern in Fig. 1, we can state that the most accurate results are obtained with the MP2/DKH computational scheme. The least accurate computational schemes are the CCSD(T)/ECP and B3LYP/ECP methods with the error of 0.106 and 0.094 Å, respectively. Similar conclusions are found by comparing experimental fundamental vibrational frequencies with the harmonic vibrational frequencies computed by us. The most accurate computational schemes are the MP2/DKH method with the mean absolute error of 7 cm^{-1} and the MP2/ECP method with the mean absolute error of 13 cm^{-1}. The largest error is again found for the CCSD(T)/ECP and B3LYP/ECP methods (32 and 33 cm^{-1}, respectively). We believe that chemical similarity between the NgMX and MNgX molecules allows for the expectation of similar trends for the MNgX molecular parameters. Therefore, we advocate using the MP2/DKH and MP2/ECP values of bond lengths and vibrational frequencies for further reference.

Certain information concerning the chemical nature of the M–Ng bond in the NgMX and MNgX species can be accessed by comparing the computed equilibrium distances with the corresponding atomic covalent and van der Waals radii.[35,43] In general one can imagine two limiting bonding schemes—covalent or van der Waals—between the M and Ng atoms. In the case of the covalent bond, the equilibrium distance r_{M-Ng} should be similar to the sum of covalent radii of M and Ng. In the case of van der Waals interaction, the equilibrium distance r_{M-Ng} should be rather similar to the sum of the van der Waals radius of Ng and the ionic radius of M^+. To verify, which of these two limiting cases describes better to the M–Ng bonding in the NgMX and MNgX molecules, we have used the following values of atomic covalent, ionic, and van der Waals radii: $r_{cov}(Ar)=0.98$ Å,[69] $r_{cov}(Kr)=1.10$ Å,[70] $r_{cov}(Xe)=1.30$ Å,[70] $r_{cov}(Cu)=1.06$ Å,[65] $r_{cov}(Ag)=1.28$ Å,[65] $r_{cov}(Au)=1.27$ Å,[65] $r_{ion}(Cu^+)=0.60$ Å,[35] $r_{ion}(Ag^+)=0.81$ Å,[35] $r_{ion}(Au^+)=0.77$ Å,[35] $r_{vdW}(Ar)=1.88$ Å,[71] $r_{vdW}(Kr)=2.00$ Å,[71] and $r_{vdW}(Xe)=2.18$ Å.[71] The calculated equilibrium bond lengths for both types of considered species, NgMX and MNgX, are much closer to the covalent bonding limit, which may suggest that the M–Ng bond has indeed a covalent character. Note that an analysis of the bonding mechanism in NgMX and MNgX in terms of molecular orbitals and molecular density was given previously by Gerry[29,31,33,35,36,38] and Ghanty.[42,43]

We have found that the CCSD(T) method is not applicable to some of the studied structures owing to an excessive multireference character of their wave functions. Such a situation occurs particularly often if the equilibrium distances between atoms are large in comparison with typically understood length of a chemical bond. A detailed analysis of a numerical failure of the CCSD(T) method is given here on the example of the AgKrCl molecule. Figure 3 shows a two-dimensional energy scan computed using the CCSD(T)/ECP method (upper left graph) for this molecule. Clearly, this graph indicates the existence of a short-distance energy minimum with $r_{Ag-Kr}=2.664$ Å and $r_{Cl-Kr}=2.768$ Å. These values agree well with analogous values predicted using B3LYP and MP2. The same graph also indicates the existence of a second low-energy region located at large atomic separations. One may naively think that this minimum corresponds to the limit of separated atoms, but short inspection of Table III shows that this limit actually lies 5.3 kcal/mol higher than the energy of short-distance minimum. The explanation of this puzzle comes from the analysis of the T_1 and D_1 diagnostics, which inform about the importance of singly excited configurations in the CCSD wave function and allow for verifying the applicability of the coupled cluster ansatz. The values of both diagnostics have large values for large interatomic separations, which clearly indicates that the CCSD(T) energies have little meaning in this region. An interesting situation happens if one incorporates the BSSE correction to the CCSD(T) potential energy surface in Fig. 1 (upper right graph). Owing to the BSSE correction, the short-distance minimum loses its stationary character and the BSSE-corrected CCSD(T) method predicts no stable bound structure for the AgKrCl molecule. We hope that this short example illustrates well the numerical problems encountered while using the CCSD(T) method in our calculations and explains the origin of triple dots in Tables I, III, V, and VI. This phenomenon and systematically poorer quality of the CCSD(T) bond lengths and harmonic vibrational frequencies in comparison with the MP2 results show most probably strong multireference character of the studied species. We are planning to perform a multireference perturbation theory study of the NgMX and MNgX compounds in the future to address this issue.

The standard counterpoise correction technique[64] used in this work to account for BSSE is normally applied to wave-function based quantum chemical methods. Here, somehow by inertia, we have applied this technique also to the B3LYP/ECP calculations. It is interesting to note that the BSSE corrections to B3LYP, which presumably correspond to deficiencies in the one-particle basis expansion of the total density, are much smaller than for the MP2 and CCSD(T) methods. For interested reader, the values of BSSE corrections for the geometry parameters, atomization energies, harmonic vibrational frequencies, and the TS structures and energies are given in Ref. 66 in Tables S I–S IV (B3LYP) and T I–T XV [CCSD(T) and MP2].

V. CONCLUSION

We have presented a detailed study of equilibrium structures, energetics, and harmonic vibrational frequencies for the noble gas containing compounds MNgX and NgMX (M=Cu, Ag, Au; X=F, Cl, Br) using a series of quantum chemical methods [MP2, CCSD(T), and B3LYP]. In agreement with earlier observations (Refs. 29–41 for NgMX and Refs. 42 and 43 for MNgX), the studied species are found to possess well-defined, partially ioniclike $(MNg)^{\delta+}X^{\delta-}$ and $(NgM)^{\delta+}X^{\delta-}$ equilibrium structures. The stability of these compounds has been examined by a comparison with two possible dissociation pathways: (1) M+Ng+X, and (2) Ng+MX. We have also investigated the transition state for the reorganization reaction MNgX→Ng+MX.

Clearly, the most important aspect of our investigations is determining which of the studied molecules can actually be observed experimentally. The presented data suggest that all of the NgMX species are stable and should be observed in laboratory under proper conditions. In fact, most of these species have been already observed experimentally.[29–39] Somewhat unsatisfactory is the fact that they probably cannot be fully considered as independent chemical molecules, but rather as very stable noble gas adducts to a strongly polarized MX molecule with the bonding energy of 2–22 kcal/mol. Much more interesting from a chemical standpoint are the MNgX species. The list of the MNgX molecules that can possibly be observed in experiment is AuKrF, AuKrCl, AuKrBr, CuXeF, AgXeF, AuXeF, AuXeCl, and AuXeBr. These structures possess large enough energy barriers that may ensure their kinetic stability and would prevent their dissociation to Ng+MX. Our results show that all the considered argon-containing MNgX compounds are kinetically unstable or very weakly bound. The MArX molecule that has the largest chance to be detected experimentally is AuArF. We believe that experimental observation of these molecules should be possible under cryogenic conditions in solid noble gas matrices or in molecular crossed-beam experiments.

ACKNOWLEDGMENTS

This research is supported by the National Science Council of Taiwan (NSC96-2113-M-009-022), Ministry of Education (MOE-ATU project), and National Center for High-Performance Computing (NCHC), Hsinchu, Taiwan.

[1] M. W. Travers, *Life of Sir William Ramsay* (E. Amold, London, 1956).
[2] P. Laszlo and G. J. Schrobilgen, Angew. Chem., Int. Ed. Engl. **27**, 479 (1988).
[3] N. Bartlett, Proc. Chem. Soc., London 218 (1962).
[4] N. N. Greenwood and A. Earnshaw, *Chemistry of the Elements* (Butterworth-Heinemann, Oxford, 2001), p. 888.
[5] P. R. Fields, L. Stein, and M. H. Zirin, J. Am. Chem. Soc. **84**, 4164 (1962).
[6] L. Stein, Science **175**, 1463 (1972).
[7] J. J. Turner and G. C. Pimentel, Science **31**, 974 (1963).
[8] J. Lundell J, G. M. Chaban, and R. B. Gerber, Chem. Phys. Lett. **331**, 308 (2000).
[9] L. Khriachtchev, M. Pettersson, N. Runeberg, J. Lundell, and M. Räsänen, Nature (London) **406**, 874 (2000).
[10] M. Pettersson, J. Lundell, and M. Räsänen, J. Chem. Phys. **102**, 6423 (1995).
[11] M. Pettersson, J. Lundell, and M. Räsänen, J. Chem. Phys. **103**, 205 (1995).
[12] M. Pettersson, J. Lundell, L. Khriachtchev, and M. Räsänen, J. Chem. Phys. **109**, 618 (1998).
[13] M. Pettersson, L. Khriachtchev, A. Lignell, and M. Räsänen, J. Chem. Phys. **116**, 2508 (2002).
[14] T.-Y. Lin, J.-B. Hsu, and W.-P. Hu, Chem. Phys. Lett. **402**, 514 (2004).
[15] A. Cohen, J. Lundell, and R. B. Gerber, J. Chem. Phys. **119**, 6415 (2003).
[16] T.-H. Li, C.-H. Mou, H.-R. Chen, and W.-P. Hu, J. Am. Chem. Soc. **127**, 9241 (2005).
[17] G. Frenking, Nature (London) **406**, 836 (2000).
[18] R. B. Gerber, Annu. Rev. Phys. Chem. **55**, 55 (2004).
[19] M. W. Wong, J. Am. Chem. Soc. **122**, 6289 (2000).
[20] S. Borocci, N. Bronzolino, and F. Grandinetti, Chem. Phys. Lett. **406**, 179 (2005).
[21] J. H. Holloway and E. G. Hope, Adv. Inorg. Chem. **46**, 51 (1999).
[22] J. F. Lehmann, H. P. A. Mercier, and G. J. Schrobilgen, Coord. Chem. Rev. **233**, 1 (2002).
[23] M. Tramšek and B. Žemva, Acta Chim. Slov. **53**, 105 (2006).
[24] W. Grochala, Chem. Soc. Rev. **36**, 1632 (2007).
[25] S. Seidel and K. Seppelt, Science **290**, 117 (2000).
[26] W.-P. Hu and C.-H. Huang, J. Am. Chem. Soc. **123**, 2340 (2001).
[27] P. X. Zhang, Y. F. Zhao, F. Y. Hao, and X. Y. Li, Int. J. Quantum Chem. **108**, 937 (2008).
[28] P. X. Zhang, Y. F. Zhao, F. Y. Hao, G. H. Zhang, X. D. Song, and X. Y. Li, Mol. Phys. **106**, 1007 (2008).
[29] L. M. Reynard, C. J. Evans, and M. C. L. Gerry, J. Mol. Spectrosc. **206**, 33 (2001).
[30] C. J. Evans and M. C. L. Gerry, J. Chem. Phys. **112**, 1321 (2000).
[31] C. J. Evans and M. C. L. Gerry, J. Chem. Phys. **112**, 9363 (2000).
[32] C. J. Evans, A. Lesarri, and M. C. L. Gerry, J. Am. Chem. Soc. **122**, 6100 (2000).
[33] C. J. Evans, D. S. Rubinoff, and M. C. L. Gerry, Phys. Chem. Chem. Phys. **2**, 3943 (2000).
[34] N. R. Walker, L. M. Reynard, and M. C. L. Gerry, J. Mol. Struct. **612**, 109 (2002).
[35] J. M. Thomas, N. R. Walker, S. A. Cooke, and M. C. L. Gerry, J. Am. Chem. Soc. **126**, 1235 (2004).
[36] S. A. Cooke and M. C. L. Gerry, Phys. Chem. Chem. Phys. **6**, 3248 (2004).
[37] J. M. Michaud, S. A. Cooke, and M. C. L. Gerry, Inorg. Chem. **43**, 3871 (2004).
[38] S. A. Cooke and M. C. L. Gerry, J. Am. Chem. Soc. **126**, 17000 (2004).
[39] J. M. Michaud and M. C. L. Gerry, J. Am. Chem. Soc. **128**, 7613 (2006).
[40] L. Belpassi, I. Infante, F. Tarantelli, and L. Visscher, J. Am. Chem. Soc. **130**, 1048 (2008).
[41] C. C. Lovallo and M. Klobukowski, Chem. Phys. Lett. **368**, 589 (2003).
[42] T. K. Ghanty, J. Chem. Phys. **123**, 074323 (2005).
[43] T. K. Ghanty, J. Chem. Phys. **124**, 124304 (2006).
[44] D. Andrae, U. Haussermann, M. Dolg, H. Stoll, and H. Preuss, Theor. Chim. Acta **77**, 123 (1990).
[45] A. Nicklass, M. Dolg, H. Stoll, and H. Preuss, J. Chem. Phys. **102**, 8942 (1995).
[46] J. M. L. Martin and A. Sundermann, J. Chem. Phys. **114**, 3408 (2001).
[47] T. H. Dunning, Jr., J. Chem. Phys. **90**, 1007 (1989).
[48] D. E. Woon and T. H. Dunning, Jr., J. Chem. Phys. **98**, 1358 (1993).
[49] R. A. Kendall, T. H. Dunning, Jr., and R. J. Harrison, J. Chem. Phys. **96**, 6769 (1992).
[50] A. K. Wilson, D. E. Woon, K. Peterson, and T. H. Dunning, Jr., J. Chem. Phys. **110**, 7667 (1999).
[51] M. Reiher and A. Wolf, J. Chem. Phys. **121**, 2037 (2004).
[52] M. Reiher and A. Wolf, J. Chem. Phys. **121**, 10945 (2004).
[53] B. O. Roos, R. Lindh, P.-Å. Malmqvist, V. Veryazov, and P.-O. Widmark, J. Phys. Chem. A **109**, 6575 (2005).
[54] Basis sets are available online at http://www.teokem.lu.se/molcas/basis/70/ANO-RCC.txt

[55] N. Douglas and M. Kroll, Ann. Phys. **82**, 89 (1974).
[56] B. Hess, Phys. Rev. A **33**, 3742 (1986).
[57] K. Raghavachari, G. W. Trucks, J. A. Pople, and M. Head-Gordon, Chem. Phys. Lett. **157**, 479 (1989).
[58] C. Møller and M. S. Plesset, Phys. Rev. **46**, 618 (1934).
[59] W. Kohn and L. J. Sham, Phys. Rev. **140**, A1133 (1965).
[60] A. D. Becke, J. Chem. Phys. **98**, 5648 (1993).
[61] C. Lee, W. Yang, and R. G. Parr, Phys. Rev. B **37**, 785 (1988).
[62] M. J. Frisch, G. W. Trucks, H. B. Schlegel *et al.*, GAUSSIAN 03, revision A.1, Gaussian, Inc., Pittsburgh, PA, 2003.
[63] MOLPRO is a package of *ab initio* programs written by H. J. Werner and P. J. Knowles with contributions from R. D. Amos *et al.*
[64] S. F. Boys and F. Bernardi, Mol. Phys. **19**, 553 (1970).
[65] P. Pyykkö, Chem. Rev. (Washington, D.C.) **88**, 563(1988), particularly pp. 573–577.
[66] See EPAPS Document No. E-JCPSA6-129-612848 for 19 tables (TI-TXV and SI-SIV) and a figure giving additional details of our calculations for MNgX and NgMX. The tables display the magnitude of the BSSE corrections and the figure shows the IRC pathway for the MNgX $\rightarrow$Ng+MX reorganization reaction together with the change of interatomic distances during the reaction. The data is presented in the PDF format. For more information on EPAPS, see http://www.aip.org/pubservs/epaps.html.
[67] T. Takayanagi, T. Asakura, K. Takahashi, Y. Taketsugu, T. Taketsugu, and T. Noro, Chem. Phys. Lett. **446**, 14 (2007).
[68] *Structure Data of Free Polyatomic Molecules*, edited by K. Kuchitsu, Landolt-Börnstein Series, Vol. II/28B (Springer, Berlin, 2006).
[69] P. Pyykkö, Science **290**, 64 (2000).
[70] N. Bartlett and F. O. Sladky, in *Comprehensive Inorganic Chemistry*, edited by J. C. Bailar, H. J. Emeléus, R. Nyholm, and A. F. Trotman-Dickenson (Pergamon, Oxford, 1973), pp. 213–330.
[71] P. Pyykkö, Chem. Rev. (Washington, D.C.) **97**, 597 (1997).